

## Collision dynamics in electron-capture processes with excitation

M. S. Schöffler,<sup>1,2,\*</sup> J. N. Titze,<sup>1</sup> L. Ph. H. Schmidt,<sup>1</sup> T. Jahnke,<sup>1</sup> O. Jagutzki,<sup>1</sup> H. Schmidt-Böcking,<sup>1</sup> and R. Dörner<sup>1</sup>

<sup>1</sup>*Institut für Kernphysik, University Frankfurt, Max-von-Laue-Str. 1, 60438 Frankfurt, Germany*

<sup>2</sup>*Lawrence Berkeley National Laboratory, Berkeley, California 94720, USA*

(Received 25 August 2009; published 6 October 2009)

We have measured the projectile scattering-angle dependency for various electronic final states for single-electron capture in p+He and <sup>3</sup>He<sup>+</sup>+He collisions at incident energies between 60 and 630 keV/u. We find pronounced peak structures in the scattering-angle dependence of some of the ratios of different capture channels. We interpret this as experimental evidence that an excitation process of the target is caused by a transverse momentum transfer that leads to an additional projectile deflection.

DOI: [10.1103/PhysRevA.80.042702](https://doi.org/10.1103/PhysRevA.80.042702)

PACS number(s): 34.50.Fa, 34.70.+e

### I. INTRODUCTION

Despite more than 50 years of experimental and theoretical studies, electron-capture processes are still an active field of ion atom collisions. In particular, those processes where more than one active electron is involved are still not sufficiently understood (see [1] for a recent review). From an experimental point of view, single-electron transfer has at least two interesting facets. First, it can be used as a tool for spectroscopy. Energy gain spectroscopy [2,3] and the related experiments in inverse kinematics which exploit the recoil ion longitudinal momentum [4,5] for  $Q$ -value determination (change in the electron binding energies) give access to the energy levels of highly charged species [6] and to energy levels that do not decay radiatively. These are difficult to access by other spectroscopic techniques. Second, the dynamics of the transfer process itself is of fundamental interest since it combines electron-electron dynamics, correlation, and questions of few-body momentum exchange. The type of electron transfer dynamics changes with projectile velocity  $v_p$ . At high velocities, nonradiative transfer proceeds via an internal atomic double-scattering process, which accelerates one of the target electrons to projectile velocity. This type of electron transfer is known as Thomas process. It leads to a characteristic projectile scattering angle of  $\theta_p = m_e/m_p$  mrad where  $m_p$  and  $m_e$  are the mass of the projectile and the electron, respectively [7–11]. At intermediate projectile velocities the capture occurs predominantly via an overlap of initial and final state wave function which are shifted in momentum space by the projectile velocity. This is most intuitively formulated in the Oppenheimer-Brinkmann-Kramers-approximation [12,13]. The term “velocity matching” captures this simple physical idea that only the fraction of the initial state wave function which has a forward momentum matching the projectile velocity finally contributes to the transfer process. The dynamics of electron transfer has been studied intensely over the past 50 years both theoretically and experimentally (see, e.g., [1,14,15] and references therein). In most of the theoretical studies the transfer into an excited state or the transfer combined with a target excitation of a second electron were neglected. Especially at higher

impact energies ( $E_p > 100$  keV/u), where the final state determination in experiments are difficult, the influence of excitation has not been investigated.

In recent studies, Hasan and co-workers [16] investigated the double ratio of transfer-excitation to single capture and double to single excitation cross section as a function of the projectile scattering angle in p+He collisions at  $E_p = 50$  keV. If the scattering potential would be the same for these different channels, one would expect a constant ratio of 2. Surprisingly, they found an enhancement of the ratio around  $\theta_p = 0.5$  mrad in the experimental data, which they couldn't describe as classical scattering theory. Follow-up calculations by Zapukhlyak *et al.* [17] suggested that the peak is not related to electron-electron correlations, but rather to the necessity of treating the nuclei quantum mechanically and not neglecting the heavy-particle-electron couplings. Also in the simpler ratios of double to single capture in p+He collisions between 50 and 100 keV, Schulz *et al.* found a peak around 0.6 mrad [18]. Similar peaks around 0.6 mrad have also been observed in earlier experiments by Schulz *et al.* [19] and in theory by Martin *et al.* [20], where they investigated the double to single excitation ratio for p+He collisions at 150 keV. There are also related peaks in the scattering-angle dependence of the double to single ionization ratio [21] and in the transfer ionization to single capture ratio [9]. We will discuss this in more detail in the results section.

Inspired by the pioneering work of Schulz and Zapukhlyak *et al.*, we address the question of the mechanism behind the transverse momentum exchange in capture processes with more than one active electron in a similar manner as Horsdal did for transfer ionization [9]. We investigate at which deflection angles the additional excitation happens. Therefore we measured, with final state selecting the projectile scattering angle for H<sup>+</sup> and <sup>3</sup>He<sup>+</sup> projectiles ( $A$ ) covering an energy range from  $E_p = 60$  to 630 keV/u. To simplify the discussion, we focus on the single ratios of ground-state transfer (1s-1s) to target (projectile) excitations. Our study significantly expands the energy range covered in the earlier works and explores two different projectile masses for each energy.

### II. EXPERIMENT

The momentum transfer in the capture processes of swift ions is typically very small compared to the projectile mo-

\*schoeffler@atom.uni-frankfurt.de

mentum. Since there are only two particles in the initial and final state, projectile and recoil ion balance their momentum exchange—one compensates the other [22]. The longitudinal momentum exchange is directly related to the total  $Q$  value of the process, i.e., the final electronic state of target and projectile. Due to momentum conservation, one can either measure the longitudinal momentum component of the projectile (traditional energy loss spectroscopy) or the longitudinal momentum of the recoiling target ion. For the swift collisions investigated here, the best resolution is obtained by detecting the recoil ion momentum instead of small change on the large projectile momentum. In the present experiments ( $A^+ + \text{He} \rightarrow A^0 + \text{He}^+$  at projectile energies between 60 and 630 keV/u) we have used the COLTRIMS technique to measure both the neutral projectile ( $\text{H}^0$  or  ${}^3\text{He}^0$ ) and the recoil ion ( $\text{He}^+$ ) in coincidence (see [23–25] for some general reviews). The experiment has been performed at the 2.5 MV van de Graaff accelerator at the Institut für Kernphysik, University of Frankfurt. We used two sets of adjustable slits to collimate the beam to a size of  $0.5 \times 0.5 \text{ mm}^2$  at the target. Two sets of electrostatic deflectors are placed in front and behind the target. They were used to clean the beam from charge state impurities in front of the target and to analyze the final charge state behind the target. The neutral  $A^0$  projectiles were detected on a 40-mm position- and time-sensitive multichannel plate (MCP) detector with delay line anode for position read-out [26,27]. The target is provided by a 2-stage supersonic gas jet. At the interaction point, the gas jet has a diameter of 1.5 mm and areal density of  $5 \times 10^{11} \text{ atoms/cm}^2$ . The  $\text{He}^+$  recoil ions produced in the overlap region of gas jet and projectile beam were projected with a weak electrostatic field (4.8 V/cm) onto a 80-mm position- and time-sensitive multi channel plate detector. A three-dimensional time- and space focusing geometry was applied to maximize the resolution [28]. From the measured data, time of flight (19  $\mu\text{s}$  for  $\text{He}^+$ ) and position of impact, we extracted the initial three-dimensional momentum vector. We achieved an overall momentum resolution of 0.1 a. u. which was limited by the target temperature. Our spectrometer geometry and electric fields yielded  $4\pi$  acceptance angle for all recoil ions with momenta below 9 a. u.

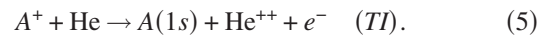
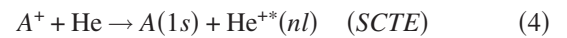
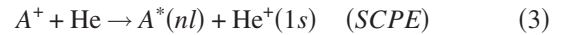
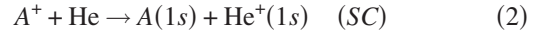
The final electronic state is encoded in the projectile energy loss ( $Q$  value) and this is related to the recoil longitudinal momentum  $p_{\parallel}$  by [5]

$$p_{\parallel} = -\frac{Q}{v_p} - \frac{v_p}{2} \quad (1)$$

In the plane perpendicular to the beam axis, we measure the scattering angle of the projectile and the transverse momentum of the recoiling ion  $p_{\perp}$ . By momentum conservation they must add to zero. We used this for background suppression. For the data presented below we deduced the scattering angle from the recoil ion transverse momentum, which has a much better momentum resolution in our setup. By gating on the different longitudinal momenta of the recoil ion, we were able to extract the scattering angles for different final electronic states [29]. The small background contribution, mainly from single ionization, has been subtracted.

### III. RESULTS AND DISCUSSION

To avoid molecular interference effects (example see [30]) during the electron transfer, the incident projectile energies are chosen above the classical Bohr velocity. We concentrate on scattering angles, below 1.5 mrad which account for about 90% of the total cross section. With our kinematically complete data set, we could determine the projectile scattering-angle dependency for single-electron capture to the ground-state (SC), transfer to an excited state of the projectile (SCPE) and capture accompanied with target excitation (SCTE) and transfer ionization (TI)



Here,  $A$  denotes our p or  $\text{He}^+$  projectile. For the excited states ( $n=2,3,\dots$ ), we do not resolve the individual  $n$  and hence sum overall ( $n \geq 2$ ). To unravel the dynamical process responsible for the excitation or ionization process, we compare the single differential cross-section  $d\sigma/d\theta_p$  of excitation with ground-state transfer

$$R_{PE} = \frac{SCPE}{SCPE + SC} \quad (6)$$

$$R_{TE} = \frac{SCTE}{SCTE + SC} \quad (7)$$

$$R_{TI} = \frac{TI}{TI + SC}. \quad (8)$$

These ratios show the probability for an additional excitation or ionization at a given scattering angle.

Capture into an excited state of the projectile proceeds in leading order as a one-step process. Capture with target excitation or ionization in contrast requires a second (independent) interaction with the projectile or a mediation by electron-electron-correlation.

For better comparison of both projectiles (p and  $\text{He}^+$ ), we display scaled scattering angles  $\theta'_p = \theta_p \cdot m$ . The advantage of this scaling is that the maximum scattering angle of the projectile at an electron is for all projectile masses at  $\theta'_p = 0.55 \text{ mrad} \cdot \text{amu}$  and the Thomas process can be found for all masses at  $0.47 \text{ mrad} \cdot \text{amu}$ .

Before going into detail, we briefly discuss the known mechanisms causing the projectile deflection for the swift low charge collisions under investigation here.

For ionization, it is well-established that scattering to angles below 0.55 mrad has a major contribution from the momentum exchange between the projectile and the active electron [31–35]. The maximum deflection angle of a projectile scattering at a resting electron is  $0.55 \text{ mrad/amu}$  (projectile mass in amu). Hence, for these small scattering angles, very large impact parameters can contribute since the deflec-

tion does not require a momentum transfer to the target nucleus. Larger scattering angles, however, require strong nucleus-nucleus interaction (Rutherford scattering) and therefore result from smaller impact parameters. While for ionization it is obvious that a binary knock-off of an electron leads to a deflection of the projectile, it might be surprising that for single capture a similar behavior is found. The scattering-angle dependence of single capture shows a steep decrease up to 0.55 mrad/amu and levels off to the much flatter slope given by the Rutherford scattering of the projectile at the target nucleus (see [5,29,36] for experiments and Belkic and Salin [37] for a theoretical proof that small angle deflection is caused by momentum transfer from the electron that is captured).

A second ionizing interaction, following single ionization or capture, as in double ionization and transfer ionization respectively, leads to an additional deflection of the projectile. Since in total, two electrons are involved, a scattering angle of up to 1.1 mrad/amu can be reached without the necessity of a momentum exchange with the target nucleus. As a consequence, the scattering-angle dependence of the ratio of double to single ionization shows a distinct peak between 0.55 mrad and 1.1 mrad [21,38]. Similarly, a distinct peak is caused in the scattering-angle dependence of the ratio of transfer ionization to single capture [9,39].

### A. Target excitation

At first we focus on the case, where one electron is captured and the remaining target electron is excited or ionized.

This additional target excitation or ionization can either be induced by a shake-up or shake-off process or an additional projectile-electron interaction [40]. We term these “knock-up” (in energy) or “knock-off.” For the shake-up mechanism, no further interaction with the projectile takes place. One would hence expect that the shake-up probability and therefore  $R_{TE}$  is independent of the scattering angle. The knock-up/knock-off mechanism in contrast can be expected to lead to an additional transverse momentum exchange.

Our data (Fig. 1) for the ratio  $R_{TE}$  for proton and  $\text{He}^+$  projectiles show a very similar shape at all different beam energies from 60 to 630 keV/u. There is a strong scattering-angle dependence which clearly rules out shake-up as the excitation mechanism, especially at lower energies. The pronounced peak around  $\theta'_p=0.5$  mrad·amu, shifts, with higher projectile velocities to smaller angles.

For comparison, we also show our measured ratio of transfer ionization to single capture in Fig. 2. The structure as well as the mass and projectile energy dependence is very similar to the one seen in Fig. 1. Our data for  $R_{TI}$  are in good agreement with results in the literature [8].

The striking similarity between  $R_{TE}$  and  $R_{TI}$  suggest that the observed peak structure in  $R_{TE}$  has the same origin as the well-understood peak in  $R_{TI}$ . This is also in accord with the reasonable expectation of continuity across the threshold from processes, which populate states below to those which populate states above the continuum threshold. Such continuity across the threshold has, for example, been seen for single capture to excited states [41].

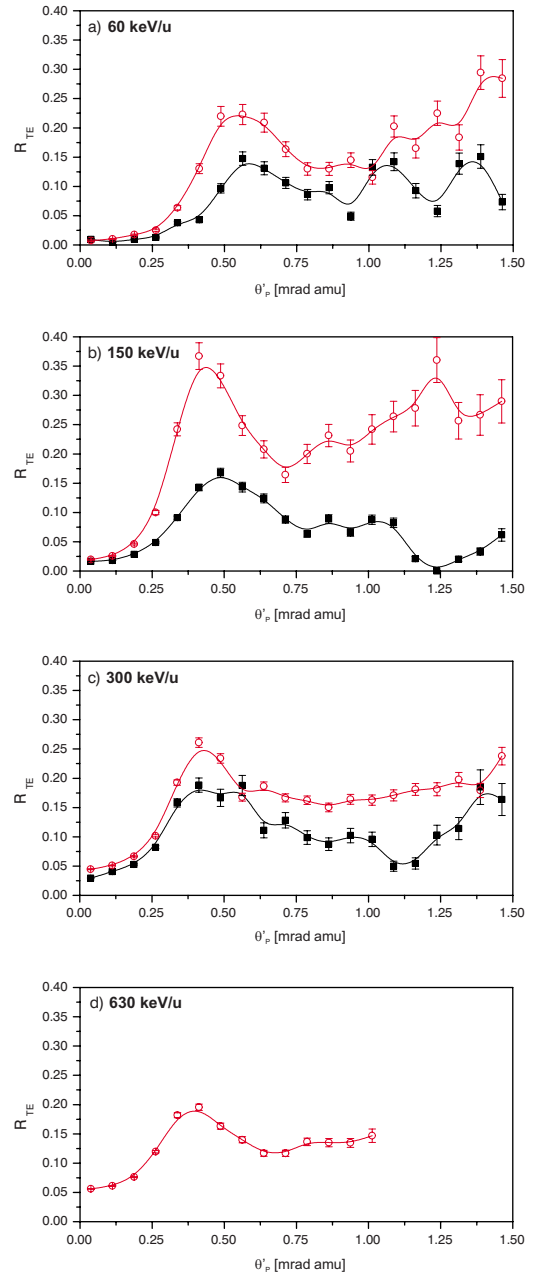


FIG. 1. (Color online) Ratio  $R_{TE}$  of transfer excitation and ground-state transfer of the differential cross-sections  $d\sigma/d\theta'_p$  in  $p + \text{He}$  and  $\text{He}^+ + \text{He}$  collisions at projectile energies of 60–630 keV/u. Black squares represent data for proton, and the red circles for  $\text{He}^+$  impact. All error bars show the statistical standard deviations. Scattering angles for  ${}^3\text{He}^+$  are multiplied by their mass to be comparable with the proton data. The line is a  $B$ -spline fit to guide the eye.

As outlined above, the origin of the peak in  $R_{TI}$  results from the fact that the single capture lead to scattering angles up to 0.55 mrad/amu—caused by the transverse momentum of the captured electron—while for TI, the second electron, which goes to the continuum, can lead to a further deflection of the projectile [39]. In analogy for SCTE one may argue that the knock-up of an electron occurs via a momentum exchange with the projectile. This is particularly intuitive if one considers the electronic wave functions in momentum

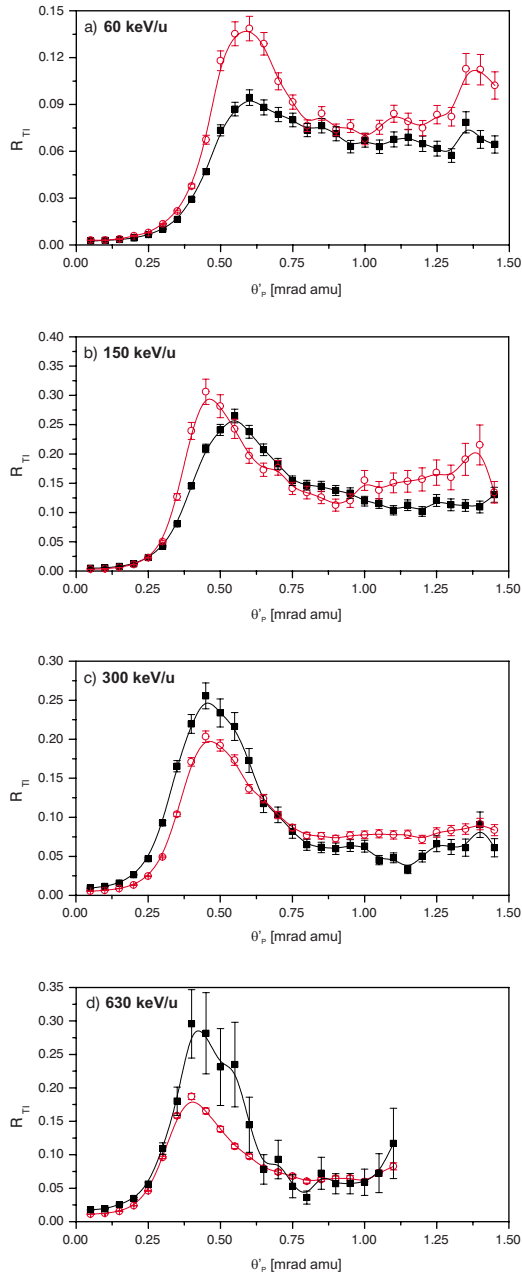


FIG. 2. (Color online) Ratio  $R_{TI}$  of transfer ionization and ground-state transfer of the differential cross-sections  $d\sigma/d\theta'_p$  in  $p+\text{He}$  and  $\text{He}^++\text{He}$  collisions at projectile energies of 60–630 keV/u. Black squares represent data for proton, and the red circles for  $\text{He}^+$  impact. All error bars show the statistical standard deviations. Scattering angles for  ${}^3\text{He}^+$  are multiplied by their mass to be comparable with the proton data. The line is a  $B$ -spline fit to guide the eye.

space. The initial ground-state wave function has a much broader profile than the excited final state. The overlap of both is what would lead to shake-up. It is very small in the present case. To effectively achieve a transition from one to the other, the momentum must be compensated by the projectile, where it leads to additional deflection eventually producing the peak in  $R_{TE}$ .

An alternative source of the observed peak would be a Thomas-type process. In a classical electron-electron-

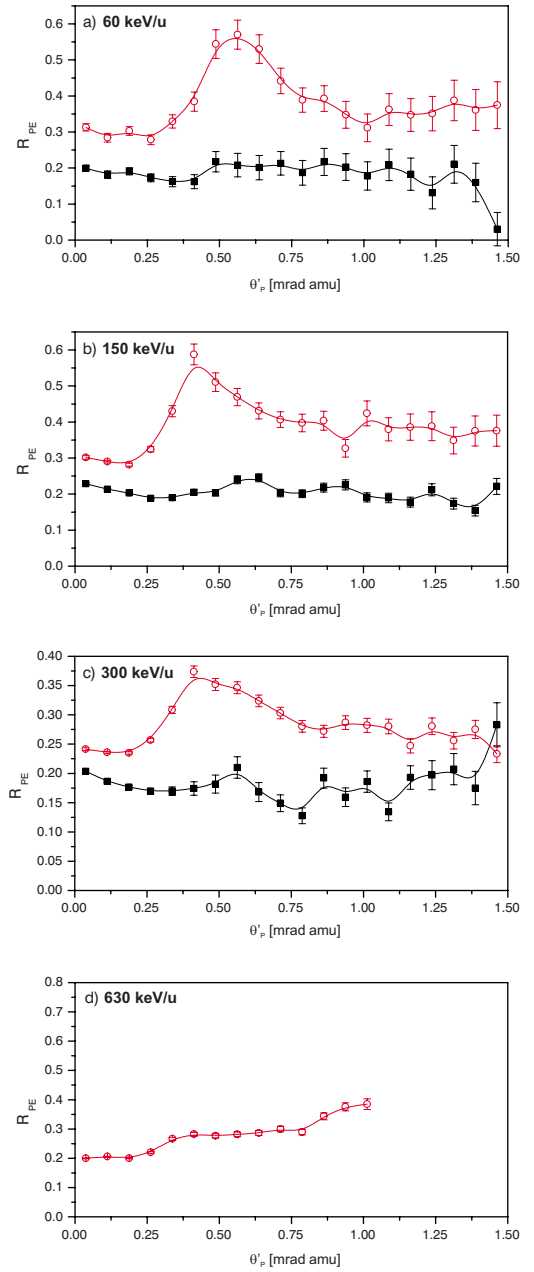


FIG. 3. (Color online) Ratio  $R_{PE}$  of electron capture into an excited state of the projectile and ground-state transfer of the differential cross-sections  $d\sigma/d\theta'_p$  in  $p+\text{He}$  and  $\text{He}^++\text{He}$  collisions at projectile energies of 60–630 keV/u. Black squares represent data for proton, and the red circles for  $\text{He}^+$  impact. All error bars show the statistical standard deviations. Scattering angles for  ${}^3\text{He}^+$  are multiplied by their mass to be comparable with the proton data. To guide the eyes  $B$ -splines connect the different points.

Thomas-process (see [8,42]), the projectile scatters  $45^\circ$  at a target electron and then scatters at a second target electron again  $45^\circ$ . In final state, one electron is accelerated to projectile velocity and captured, while the second electron is emitted perpendicularly to the incoming projectile. If one goes beyond these idealized conditions presuming a larger impact parameter, the target electron would gain less momentum (energy) would be found in an excited target state. Data at only one projectile energy cannot distinguish be-

tween the knock-up scenario and the Thomas-like processes. These would differ merely by a few hundredths of mrad, which are broadened by the initial electron momentum distribution. However the two processes would show a different projectile velocity dependency. As the electron transfer via Thomas process plays a significant role only at extreme high impact energies (above 7.5 MeV/u) [11], this process is very unlikely to produce the observed peak.

To summarize, we suppose, that the additional target excitation proceeds via a peripheral momentum exchange between the projectile nucleus and the remaining target electron to be excited. The electron gains enough energy to get excited, but not enough to escape to the continuum.

### B. Projectile excitation

Instead of an additional excitation of the target, the capture electron itself can end up in an excited state of the projectile. For proton impact and  $H^0$  in the final state this does not require a second interaction. For an  $He^+$  projectile leading to excited He however, there are two possible scenarios: either the transferred electron is captured to the excited state, in which case no second interaction is necessary and we have the same situation as for proton impact. Alternatively the capture might lead in a first step to the ground state and the second electron is then knocked up in second interaction to an excited state. In this case, the situation is similar to target excitation.

Our data shown in Fig. 3 clearly distinguish each scenario. For proton impact, we observe no peak in the 0 to 0.5 mrad region but a slight overall decrease with scattering angle. This can be qualitatively understood by considering that the classical Bohr radii of excited states are larger than the ground-state radius. Accordingly, the electron transfer can happen at larger impact parameter and hence to smaller scattering angles. For  $He^+$  impact at the lowest impact energies a clear peak arises, similar to Fig. 1. Also, the peak height and position shifts to smaller angles and decreases with the projectile energy. This clearly shows that the projectile excitation is not the result of a direct one step capture to an excited state as for proton impact but rather involves a

second interaction (with the target system), which leads to an additional deflection.

### IV. CONCLUSIONS

In conclusion, we have measured single-electron transfer in proton-helium and  $He^+$ -helium collisions in the energy range of 60 to 630 keV/u and investigated the dynamics of additional excitation processes (target and projectile) by focusing on their scattering-angle dependency. We found that capture with target excitation can be considered a two-step process, where excitation is induced by impact excitation (knock-up). For excitation of the projectile we find for protons that the projectile excitation happens directly during the capture process, while for  $He^+$  projectiles the capture proceeds to the ground state and a second step leads to excitation by knock-up. The momentum transfer in this knock-up of a projectile electron leads to a peak in the cross-section ratios exactly like the knock-up for target excitation. The results suggest that a quantum mechanical treatment of elastic projectile and target nucleus scattering, as proposed by Schulz [18], is not necessary to describe the observed peak structure around 0.5 mrad for the simple ratio of target excitation and single-electron capture. Moreover, the absence of a peak in proton-Helium collisions with projectile excitation confirms this interpretation, as the nucleus-nucleus scattering should be similar and most likely independent of the electronic state interactions. Also the de Broglie wavelengths of the projectiles vary from  $5.6e-5$  a.u. ( $H^+$  60 keV/u) to  $1e-5$  a.u. ( $^3He^+$  630 keV/u), compared to  $6.1e-5$  a.u. ( $H^+$  50 keV/u) from Schulz *et al.*, quite a bit and one would expect a stronger change. But, we also have to note, that our rather simple picture gives no explanation for the observed peak around 0.5 mrad in the double ratios, investigated by Zapukhlyak *et al.* [17].

### ACKNOWLEDGMENTS

This work was supported by DFG, the BMBF, and Roentdek GmbH. We thank T. Kirchner and M. Schulz for discussion. Also, we gratefully acknowledge the help of M. H. Prior.

- 
- [1] D. Belkic, I. Mancev, and J. Hanssen, *Rev. Mod. Phys.* **80**, 249 (2008).
  - [2] R. Mann, C. L. Cocke, A. S. Schlachter, M. Prior, and R. Marrus, *Phys. Rev. Lett.* **49**, 1329 (1982).
  - [3] R. Janev and H. Winter, *Phys. Rep., Phys. Lett.* **117**, 265 (1985).
  - [4] R. Ali, V. Frohne, C. L. Cocke, M. Stockli, S. Cheng, and M. L. A. Raphaelian, *Phys. Rev. Lett.* **69**, 2491 (1992).
  - [5] V. Mergel, R. Dörner, J. Ullrich, O. Jagutzki, S. Lencinas, S. Nüttgens, L. Spielberger, M. Unverzagt, C. L. Cocke, R. E. Olson, M. Schulz, U. Buck, E. Zanger, W. Theisinger, M. Isser, S. Geis, and H. Schmidt-Böcking, *Phys. Rev. Lett.* **74**, 2200 (1995).
  - [6] D. Fischer, B. Feuerstein, R. D. DuBois, R. Moshhammer, J. R. C. Lopez-Urrutia, I. Draganic, H. Lorch, A. N. Perumal, and J. Ullrich, *J. Phys. B* **35**, 1369 (2002).
  - [7] L. H. Thomas, *Proc. R. Soc. London, Ser. A* **114**, 561 (1927).
  - [8] E. Horsdal-Pedersen, C. L. Cocke, and M. Stockli, *Phys. Rev. Lett.* **50**, 1910 (1983).
  - [9] E. Horsdal, B. Jensen, and K. O. Nielsen, *Phys. Rev. Lett.* **57**, 1414 (1986).
  - [10] H. Vogt, R. Schuch, E. Justiniano, M. Schulz, and W. Schwab, *Phys. Rev. Lett.* **57**, 2256 (1986).
  - [11] D. Fischer, K. Stochkel, H. Cederquist, H. Zettergren, P. Reinhard, R. Schuch, A. Kallberg, A. Simonsson, and H. T. Schmidt, *Phys. Rev. A* **73**, 052713 (2006).

- [12] J. Oppenheimer, *Phys. Rev.* **31**, 349 (1928).
- [13] H. Brinkman and H. Kramers, *Proc. R. Acad. Sci. Amsterdam* **33**, 973 (1930).
- [14] D. Belkic, R. Gayet, and A. Salin, *Phys. Rep., Phys. Lett.* **56**, 279 (1979).
- [15] P. N. Abufager, P. D. Fainstein, A. E. Martinez, and R. D. Rivarola, *J. Phys. B* **38**, 11 (2005).
- [16] A. Hasan, B. Tooke, M. Zapukhlyak, T. Kirchner, and M. Schulz, *Phys. Rev. A* **74**, 032703 (2006).
- [17] M. Zapukhlyak, T. Kirchner, and A. Hasan, *Phys. Rev. A* **77**, 012720 (2008).
- [18] M. Schulz, T. Vajnai, and J. A. Brand, *Phys. Rev. A* **75**, 022717 (2007).
- [19] M. Schulz, W. T. Htwe, A. D. Gaus, J. L. Peacher, and T. Vajnai, *Phys. Rev. A* **51**, 2140 (1995).
- [20] F. Martin and A. Salin, *J. Phys. B* **28**, 1985 (1995).
- [21] J. Giese and E. Horsdal, *Phys. Rev. Lett.* **60**, 2018 (1988).
- [22] J. Ullrich, R. E. Olson, R. Dörner, V. Dangendorf, S. Kelbch, H. Berg, and H. Schmidt-Böcking, *J. Phys. B* **22**, 627 (1989).
- [23] J. Ullrich, R. Moshhammer, R. Dörner, O. Jagutzki, V. Mergel, H. Schmidt-Böcking, and L. Spielberger, *J. Phys. B* **30**, 2917 (1997).
- [24] R. Dörner, V. Mergel, O. Jagutzki, L. Spielberger, J. Ullrich, R. Moshhammer, and H. Schmidt-Böcking, *Phys. Rep., Phys. Lett.* **330**, 95 (2000).
- [25] J. Ullrich, R. Moshhammer, A. Dorn, R. Dörner, L. Schmidt, and H. Schmidt-Böcking, *Rep. Prog. Phys.* **66**, 1463 (2003).
- [26] O. Jagutzki, V. Mergel, K. Ullmann-Pfleger, L. Spielberger, U. Spillmann, R. Dörner, and H. Schmidt-Böcking, *Nucl. Instrum. Methods Phys. Res. A* **477**, 244 (2002).
- [27] O. Jagutzki, J. Lapington, L. Worth, U. Spillman, V. Mergel, and H. Schmidt-Böcking, *Nucl. Instrum. Methods Phys. Res. A* **477**, 256 (2002).
- [28] R. Dörner, V. Mergel, L. Spielberger, O. Jagutzki, S. Nüttgens, M. Unverzagt, H. Schmidt-Böcking, J. Ullrich, R. E. Olson, K. Tökesi, W. E. Meyerhof, W. Wu, and C. L. Cocke, *Nucl. Instrum. Methods Phys. Res. B* **99**, 111 (1995).
- [29] M. S. Schöffler, J. Titze, L. Ph. H. Schmidt, T. Jahnke, N. Neumann, O. Jagutzki, H. Schmidt-Böcking, R. Dörner, and I. Mančev, *Phys. Rev. A* **79**, 064701 (2009).
- [30] L. K. Johnson, R. S. Gao, R. G. Dixson, K. A. Smith, N. F. Lane, R. F. Stebbings, and M. Kimura, *Phys. Rev. A* **40**, 3626 (1989).
- [31] E. Y. Kamber, C. L. Cocke, S. Cheng, and S. L. Varghese, *Phys. Rev. Lett.* **60**, 2026 (1988).
- [32] R. Dörner, J. Ullrich, H. Schmidt-Böcking, and R. E. Olson, *Phys. Rev. Lett.* **63**, 147 (1989).
- [33] F. G. Kristensen and E. Horsdal-Pedersen, *J. Phys. B* **23**, 4129 (1990).
- [34] A. Gensmantel, J. Ullrich, R. Dörner, R. E. Olson, K. Ullmann, E. Forberich, S. Lencinas, and H. Schmidt-Böcking, *Phys. Rev. A* **45**, 4572 (1992).
- [35] T. Weber, K. Khayyat, R. Dörner, V. Mergel, O. Jagutzki, L. Schmidt, F. Afaneh, A. Gonzalez, C. L. Cocke, A. L. Landers, and H. Schmidt-Böcking, *J. Phys. B* **33**, 3331 (2000).
- [36] V. Mergel, R. Dörner, K. Khayyat, M. Achler, T. Weber, O. Jagutzki, H. J. Lüdde, C. L. Cocke, and H. Schmidt-Böcking, *Phys. Rev. Lett.* **86**, 2257 (2001).
- [37] D. Belkic and A. Salin, *J. Phys. B* **11**, 3905 (1978).
- [38] R. E. Olson, J. Ullrich, R. Dörner, and H. Schmidt-Böcking, *Phys. Rev. A* **40**, 2843 (1989).
- [39] R. Gayet and A. Salin, *Nucl. Instrum. Methods Phys. Res. B* **56-57**, 82 (1991).
- [40] K. M. Dunseath and D. S. F. Crothers, *J. Phys. B* **24**, 5003 (1991).
- [41] T. Weber, K. Khayyat, R. Dörner, V. D. Rodríguez, V. Mergel, O. Jagutzki, L. Schmidt, K. A. Müller, F. Afaneh, A. Gonzalez, and H. Schmidt-Böcking, *Phys. Rev. Lett.* **86**, 224 (2001).
- [42] V. Mergel, R. Dörner, M. Achler, K. Khayyat, S. Lencinas, J. Euler, O. Jagutzki, S. Nüttgens, M. Unverzagt, L. Spielberger, W. Wu, R. Ali, J. Ullrich, H. Cederquist, A. Salin, C. J. Wood, R. E. Olson, Dž. Belkić, C. L. Cocke, and H. Schmidt-Böcking, *Phys. Rev. Lett.* **79**, 387 (1997).